Supplementary Materials to:

β²-*homo*-Amino acid scan of μ-selective opioid tetrapeptide TAPP

by: Dagmara Tymecka*, Piotr F. J. Lipiński, Piotr Kosson and Aleksandra Misicka*

Corresponding authors: dulok@chem.uw.edu.pl; (D.T.), misicka@chem.uw.edu.pl (A.M.)

Table SM-SYN-1. Analytical data of the synthesized peptides.

No.	peptide	HPLC t_R (min)*	HPLC t_R (min)**	molecular formula	HR ESI-MS		
					calculated for $[M+H]^+$	measured for $[M+H]^+$	Diff. [ppm]
1	H-Tyr-D-Ala-Phe-Phe-NH_2 (TAPP)	20.866	18.017	$C_{30}H_{35}N_5O_5$	546.2711	546.2715	0.73
8	H-(*R*)-β^2hTyr-D-Ala-Phe-Phe-NH_2 less polar	21.160	18.672	$C_{31}H_{37}N_5O_5$	560.2867	560.2885	3.21
9	H-(*R*)-β^2h-*m*-Tyr-D-Ala-Phe-Phe-NH_2 less polar	21.831	19.240	$C_{31}H_{37}N_5O_5$	560.2867	560.2885	3.21
10	H-Tyr-(*S*)-β^2hAla-Phe-Phe-NH_2	20.059	17.340	$C_{31}H_{37}N_5O_5$	560.2867	560.2893	4.64
11	H-Tyr-D-Ala-(*R*)-β^2hPhe-Phe-NH_2	19.234	16.234	$C_{31}H_{37}N_5O_5$	560.2867	560.2879	2.14
12	H-Tyr-D-Ala-Phe-(*R*)-β^2hPhe-NH_2	20.690	18.316	$C_{31}H_{37}N_5O_5$	560.2867	560.2889	3.93
13	H-(*S*)-β^2hTyr-D-Ala-Phe-Phe-NH_2 more polar	19.585	17.019	$C_{31}H_{37}N_5O_5$	560.2867	560.2874	1.25
14	H-(*S*)-β^2h-*m*-Tyr-D-Ala-Phe-Phe-NH_2 more polar	20.039	17.711	$C_{31}H_{37}N_5O_5$	560.2867	560.2879	2.14
15	H-Tyr-(*R*)-β^2hAla-Phe-Phe-NH_2	19.496	16.876	$C_{31}H_{37}N_5O_5$	560.2867	560.2880	2.32
16	H-Tyr-D-Ala-(*S*)-β^2hPhe-Phe-NH_2	21.037	19.467	$C_{31}H_{37}N_5O_5$	560.2867	560.2879	2.14
17	H-Tyr-D-Ala-Phe-(*S*)-β^2hPhe-NH_2	20.611	18.298	$C_{31}H_{37}N_5O_5$	560.2867	560.2882	2.68

*linear gradient was applied: 3–97% B for 40 min, phase (A): 0.1% TFA in water; phase (B): 0.1% TFA in ACN.

**linear gradient was applied: 30–97% B for 30 min, phase (A): 0.1% TFA in water; phase (B): 0.1% TFA in MeOH.

Table SM-BIN-1. δOR binding affinity of the studied compounds.

No.	Compound	IC_{50} [nM][1]
		δOR[2]
1	TAPP	616
backbone expansion without changing the spatial positioning of the side-chain		
8[3]	[(*R*)-β^{2}hTyr^1]-TAPP*	>10000
9[3]	[(*R*)-β^{2}h-*m*-Tyr^1]-TAPP*	>10000
10	[(*S*)-β^{2}hAla^2]-TAPP	>10000
11	[(*R*)-β^{2}hPhe^3]-TAPP	794
12	[(*R*)-β^{2}hPhe^4]-TAPP	708
backbone expansion with changing the spatial positioning of the side-chain		
13[3]	[(*S*)-β^{2}hTyr^1]-TAPP*	>10000
14[3]	[(*S*)-β^{2}h-*m*-Tyr^1]-TAPP*	>10000
15	[(*R*)-β^{2}hAla^2]-TAPP	>10000
16	[(*S*)-β^{2}hPhe^3]-TAPP	890
17	[(*S*)-β^{2}hPhe^4]-TAPP	417

[1] IC_{50}, half-maximal inhibitory concentration mean of three determinations in duplicate. [2] Radioligand: 0.5 nM [^{3}H]DELT II. [3] Absolute configuration determined *per analogiam* to [(*R/S*)-β^{2}hPhe^1]-TAPP (see Section 2.1 in the main text for details)

Table SM-MOD-1. Descriptive summary of the binding poses predicted by docking for TAPP and the derivatives.

No	Structure	Xxx1 interactions	H-bond with Tyr148	Position of Xxx^3 side-chain	Position of Xxx^4 side-chain	Interactions of C-terminal amide
	DAMGO in 6DDF	SA1	-	n/a	SD1	n/a
1	TAPP	SA1	-	SC1	SD1	SE1
8	[(*R*)-β^2hTyr^1]-TAPP*	SA1	-	SC2	SC4	SE2
9	[(*R*)-β^2h-*m*-Tyr^1]-TAPP*	SA2	-	SC1	SD1	SE1
10	[(*S*)-β^2hAla^2]-TAPP	SA3	+	SC4	SC3	SE2
11	[(*R*)-β^2hPhe^3]-TAPP	SA4	+	to solvent	SD1	SE2
12	[(*R*)-β^2hPhe^4]-TAPP	SA4	-	SC4	SD1	SE2
13	[(*S*)-β^2hTyr^1]-TAPP*	SA5	-	SD1	SC4	to solvent
14	[(*S*)-β^2h-*m*-Tyr^1]-TAPP*	SA6	-	SC1	SD1	SE1
15	[(*R*)-β^2hAla^2]-TAPP	SA6	+	SD1	SD2	SE3
16	[(*S*)-β^2hPhe^3]-TAPP	SA7	-	SC4	SC3	solvent
17	[(*S*)-β^2hPhe^4]-TAPP	SA1	-	SC5	SD1	SE2

SA1, dispersive contacts: Ile296, His297, Val300
SA2, dispersive contacts: Met151
SA3, H-bond: Ile296 (backbone); dispersive contacts: Ile296, Val300, Ile322
SA4, H-bond: Lys233 (backbone); dispersive contacts: Val300
SA5, dispersive contacts: Ile296, Val300, Val236
SA6, H-bond: Ile296 (backbone); dispersive contacts: Val236, Ile296
SA7, H-bond: Trp293 (indole); dispersive contacts: Ile 296, Val300
SC1, dispersive contacts: Asn127, Trp318, His319
SC2, intramolecular stack $NH^+\cdots Xxx^3$
SC3, dispersive contacts: Cys217
SC4, dispersive contacts: Leu219
SC5, intramolecular stack $Xxx^4\cdots Xxx^3$
SD1, dispersive contacts: Trp133, Ile144, Cys217
SD2, dispersive contacts: Val300, Trp318
SE1, H-bond: Thr218
SE2, H-bond: Asp216
SE3, H-bond: Glu229

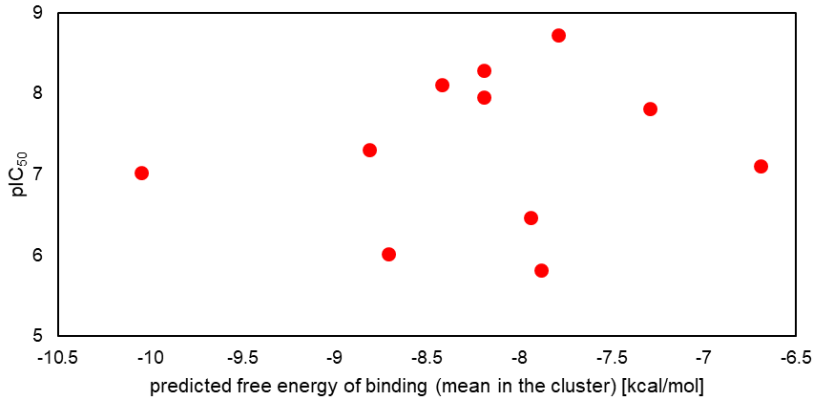

Figure SM-MOD-1. Plot of pIC_{50} against the predicted by docking free energy of binding (mean in the cluster).

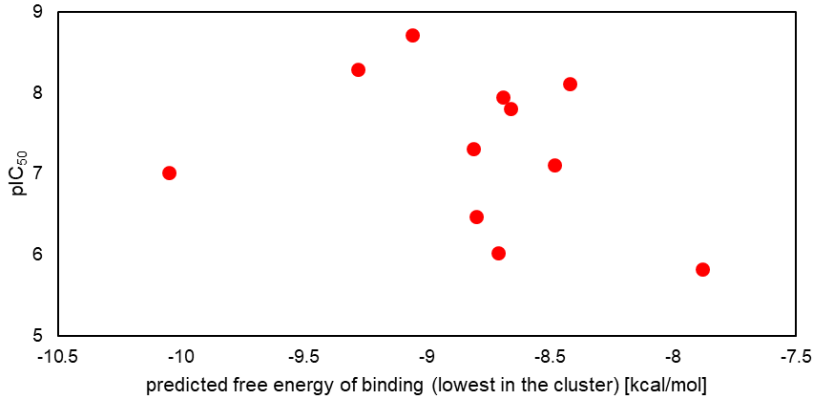

Figure SM-MOD-2. Plot of pIC_{50} against the predicted by docking free energy of binding (lowest in the cluster).

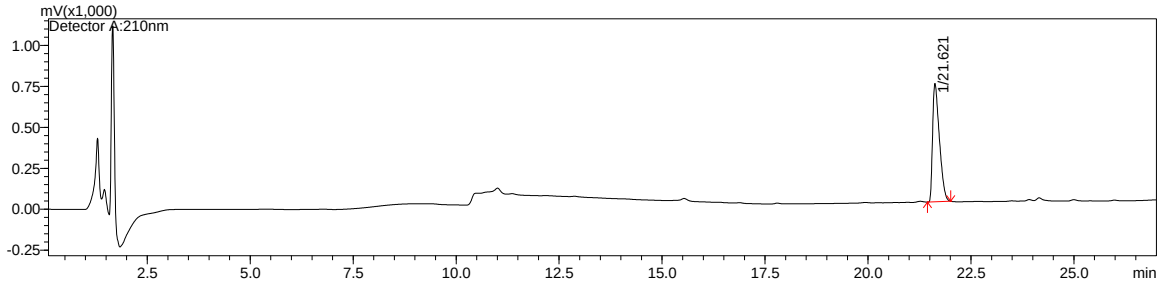

Figure SM-STAB-1. HPLC chromatogram of a TAPP (**1**) sample in human plasma, taken at the start of stability testing.

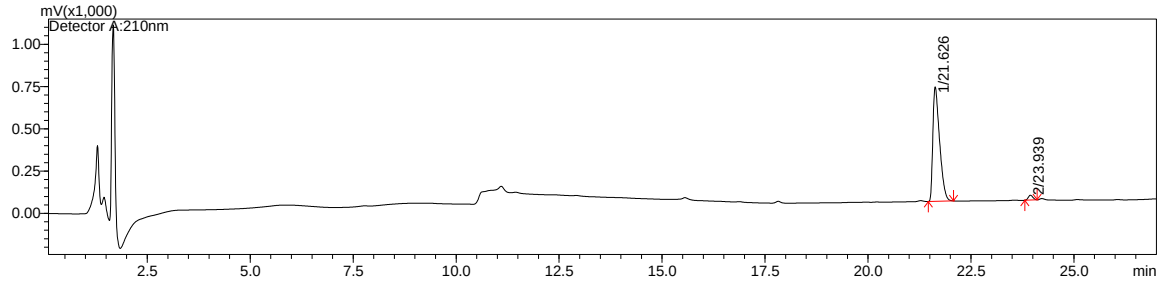

Figure SM-STAB-2. HPLC chromatogram of a TAPP (**1**) sample in human plasma, taken at 48 h of stability testing.

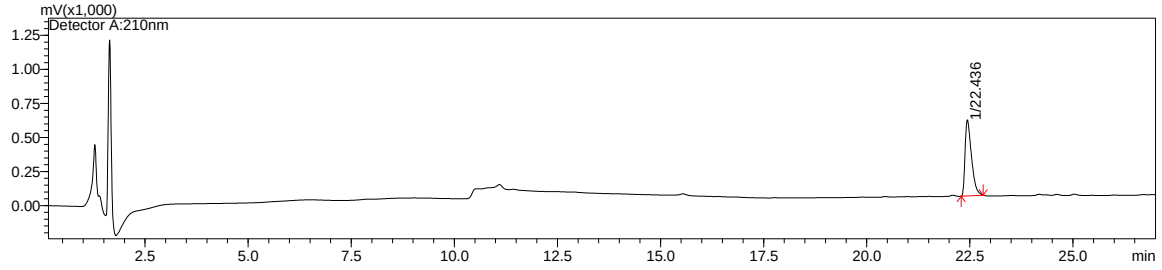

Figure SM-STAB-3. HPLC chromatogram of a [(*R*)-β^2hTyr^1]-TAPP* (**8**) sample in human plasma, taken at the start of stability testing.

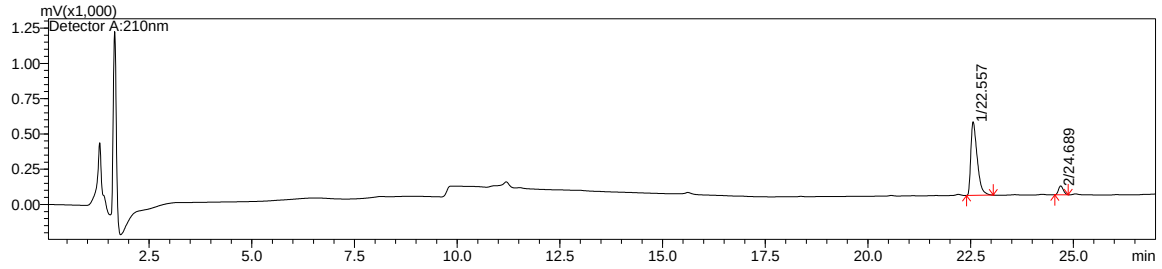

Figure SM-STAB-4. HPLC chromatogram of a [(*R*)-β^{2}hTyr^1]-TAPP* (**8**) sample in human plasma, taken at 48 h of stability testing.

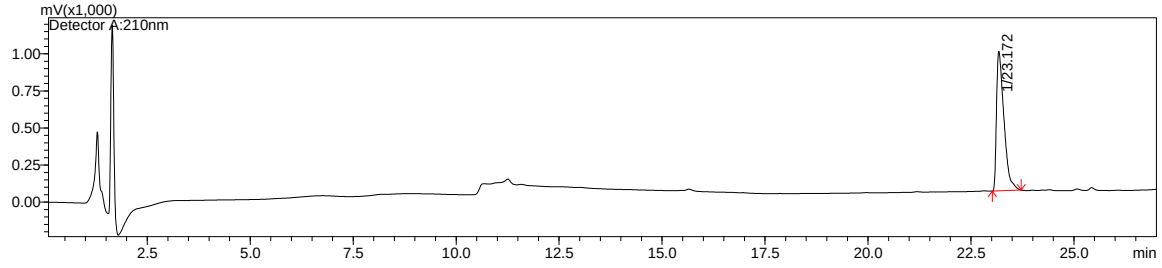

Figure SM-STAB-5. HPLC chromatogram of a [(*R*)-β^{2}h-*m*-Tyr^1]-TAPP* (**9**) sample in human plasma, taken at the start of stability testing.

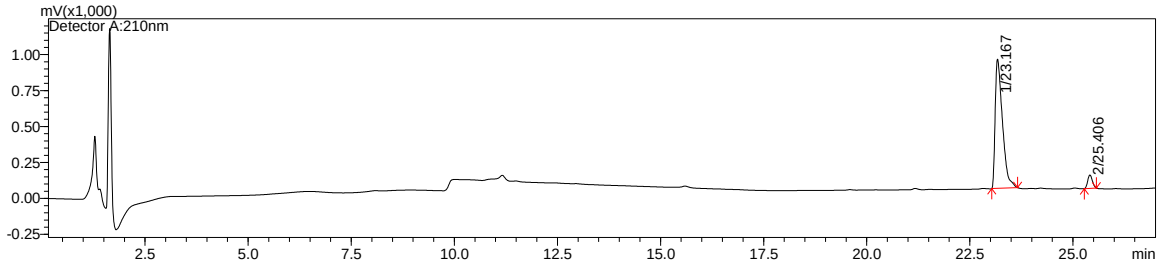

Figure SM-STAB-6. HPLC chromatogram of a [(*R*)-β^{2}h-*m*-Tyr^1]-TAPP* (**9**) sample in human plasma, taken at 48 h of stability testing.

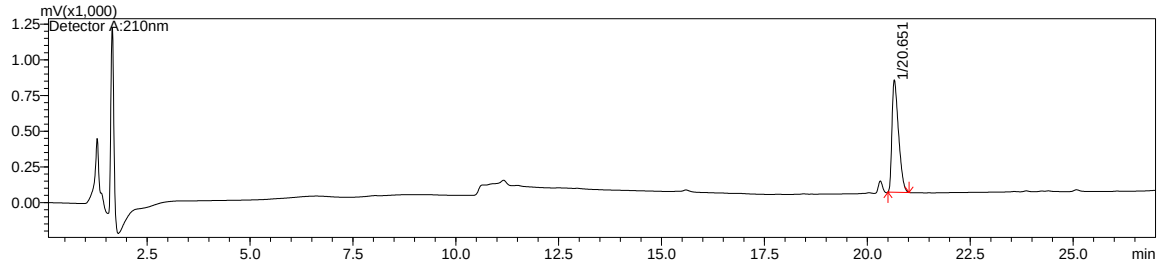

Figure SM-STAB-7. HPLC chromatogram of a [(*S*)-β^{2}hAla^2]-TAPP (**10**) sample in human plasma, taken at the start of stability testing.

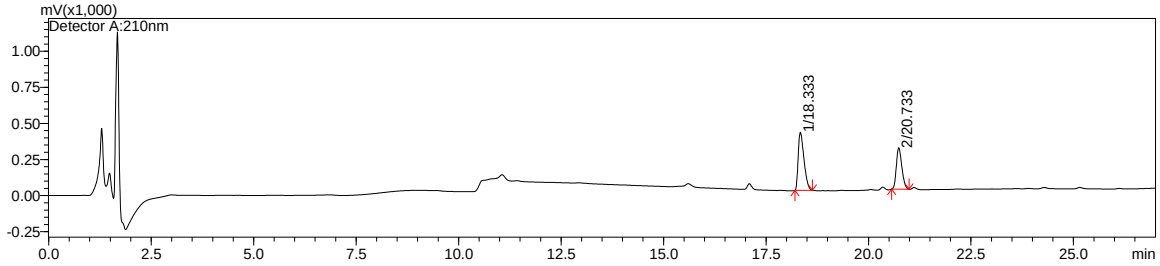

Figure SM-STAB-8. HPLC chromatogram of a [(*S*)-β^{2}hAla^2]-TAPP (**10**) sample in human plasma, taken at 4 h of stability testing.

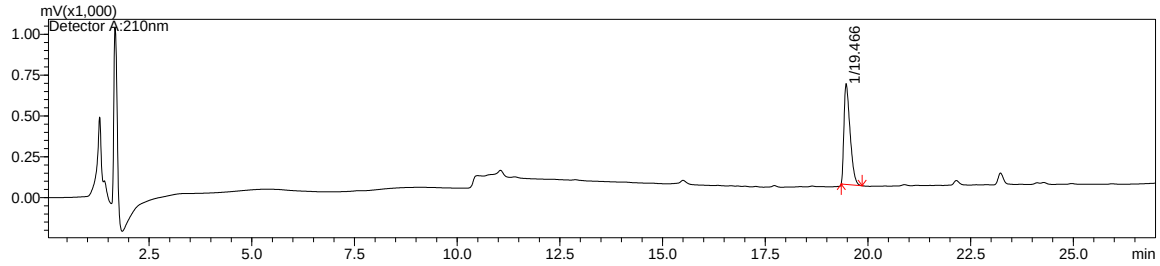

Figure SM-STAB-9. HPLC chromatogram of [(*R*)-β^{2}hPhe^3]-TAPP (**11**) sample in human plasma, taken at the start of stability testing.

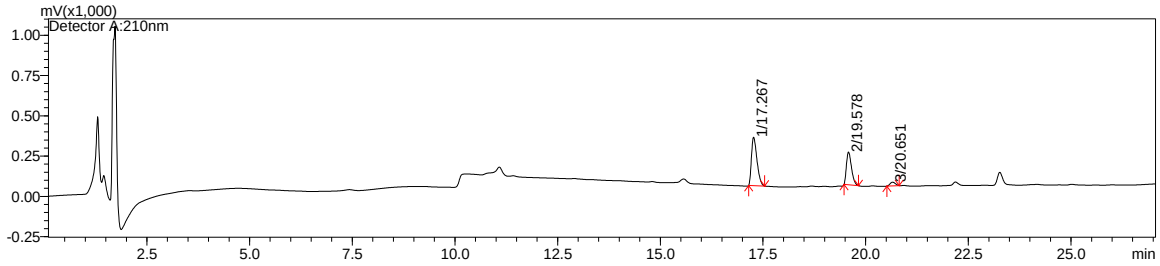

Figure SM-STAB-10. HPLC chromatogram of [(*R*)-β^{2}hPhe^3]-TAPP (**11**) sample in human plasma, taken at 48h of stability testing.

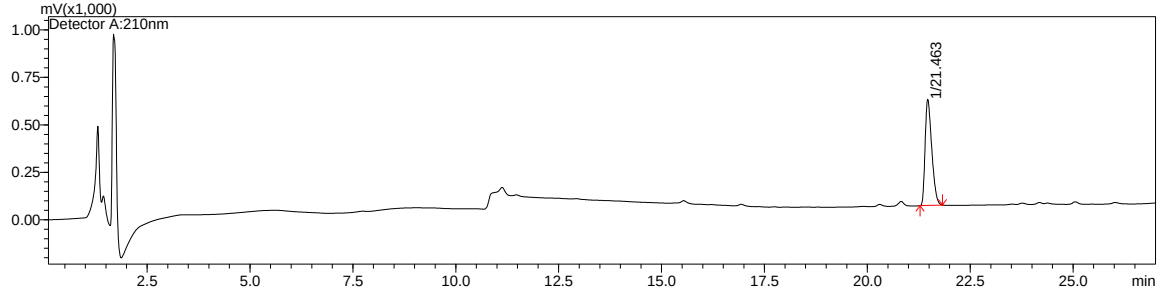

Figure SM-STAB-12. HPLC chromatogram of [(*R*)-β^{2}hPhe^4]-TAPP (**12**) sample in human plasma, taken at the start of stability testing.

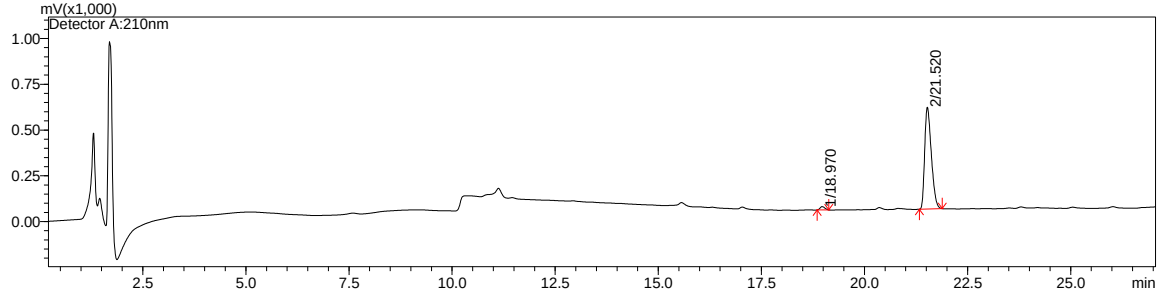

Figure SM-STAB-12. HPLC chromatogram of [(*R*)-β^{2}hPhe^4]-TAPP (**12**) sample in human plasma, taken at 48 h of stability testing.

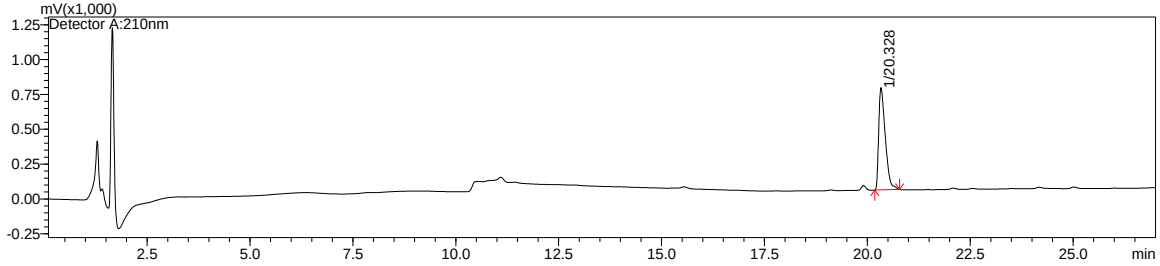

Figure SM-STAB-13. HPLC chromatogram of a [(*S*)-β^{2}hTyr^{1}]-TAPP* (**13**) sample in human plasma, taken at the start of stability testing.

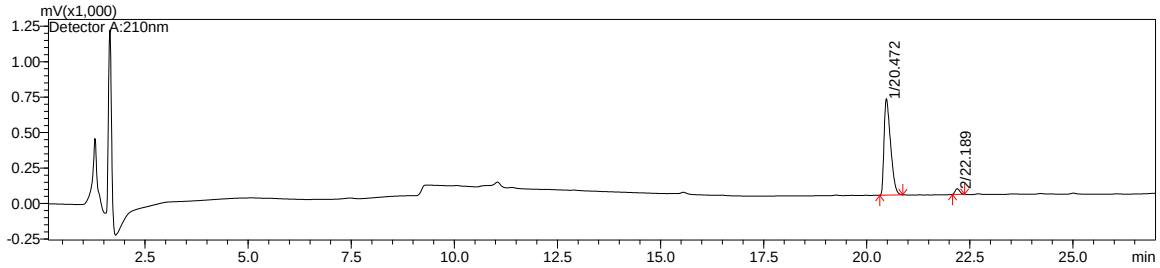

Figure SM-STAB-14. HPLC chromatogram of a [(*S*)-β^{2}hTyr^{1}]-TAPP* (**13**) sample in human plasma, taken at 48 h of stability testing.

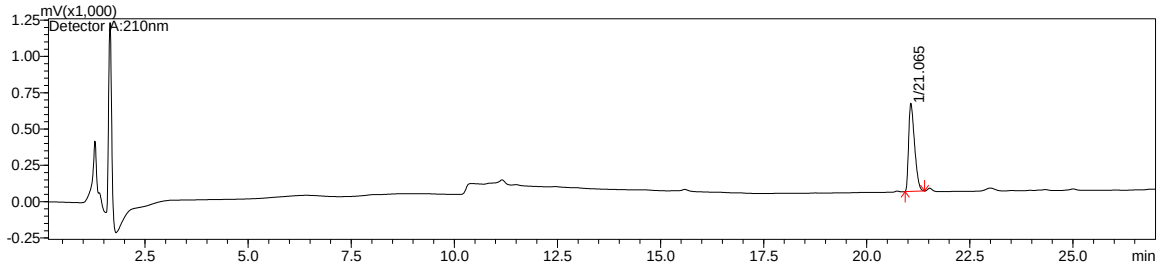

Figure SM-STAB-15. HPLC chromatogram of a [(*S*)-β^{2}h-*m*-Tyr^{1}]-TAPP* (**14**) sample in human plasma, taken at the start of stability testing.

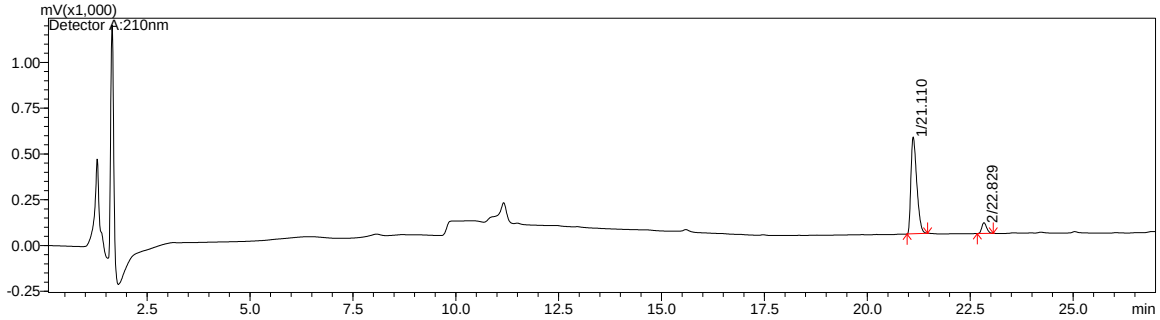

Figure SM-STAB-16. HPLC chromatogram of a [(*S*)-β^{2}h-*m*-Tyr^{1}]-TAPP* (**14**) sample in human plasma, taken at 48 h of stability testing.

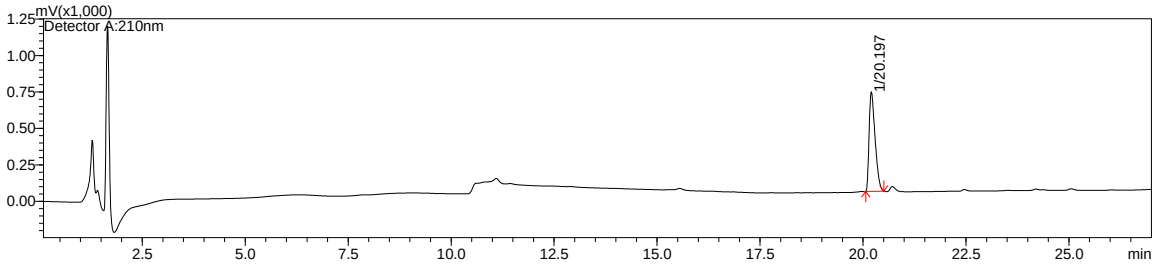

Figure SM-STAB-17. HPLC chromatogram of a [(*R*)-β^{2}hAla^2]-TAPP (**15**) sample in human plasma, taken at the start of stability testing.

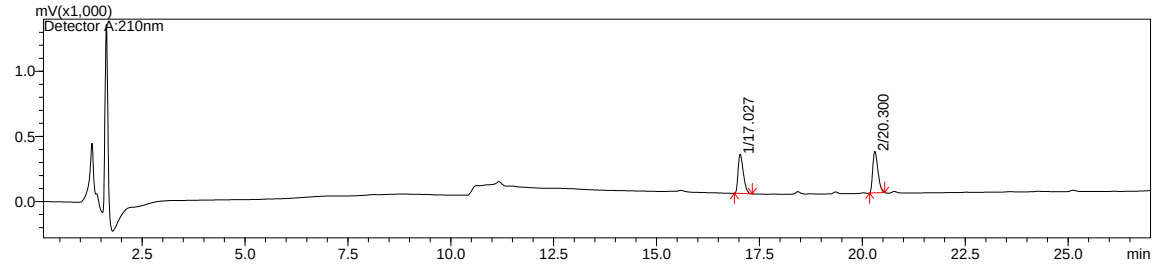

Figure SM-STAB-18. HPLC chromatogram of a [(*R*)-β^{2}hAla^2]-TAPP (**15**) sample in human plasma, taken at 4 h of stability testing.

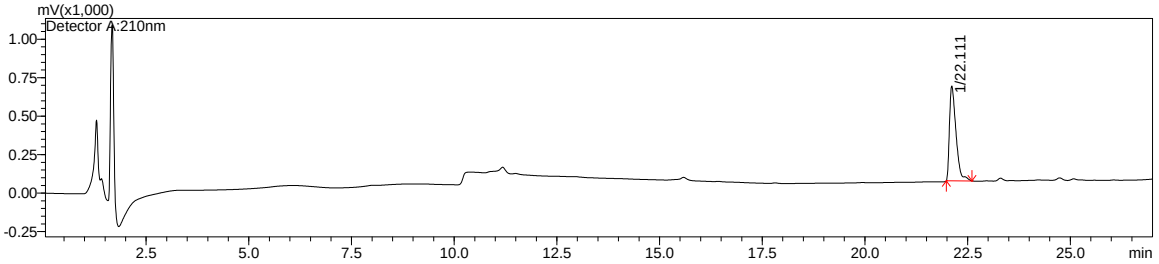

Figure SM-STAB-19. HPLC chromatogram of a [(*S*)-β^{2}hPhe^3]-TAPP (**16**) sample in human plasma, taken at the start of stability testing.

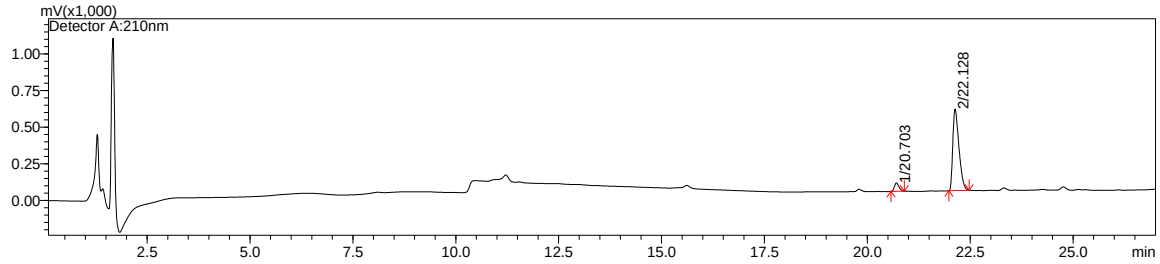

Figure SM-STAB-20. HPLC chromatogram of a [(*S*)-β^{2}hPhe^{3}]-TAPP (**16**) sample in human plasma, taken at 48 h of stability testing.

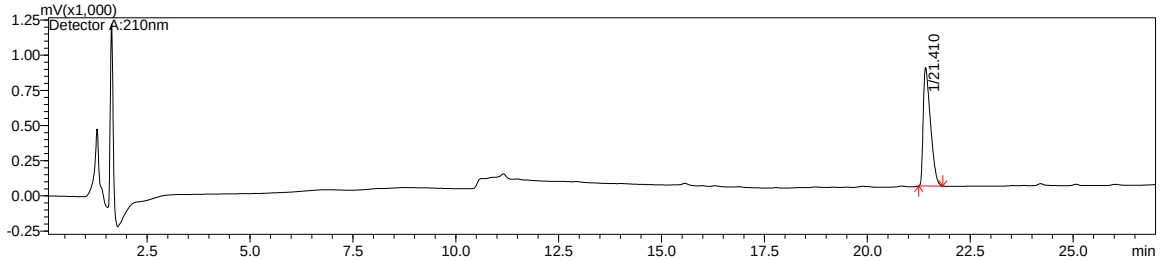

Figure SM-STAB-21. HPLC chromatogram of a [(*S*)-β^{2}hPhe^{4}]-TAPP (**17**) sample in human plasma, taken at the start of stability testing.

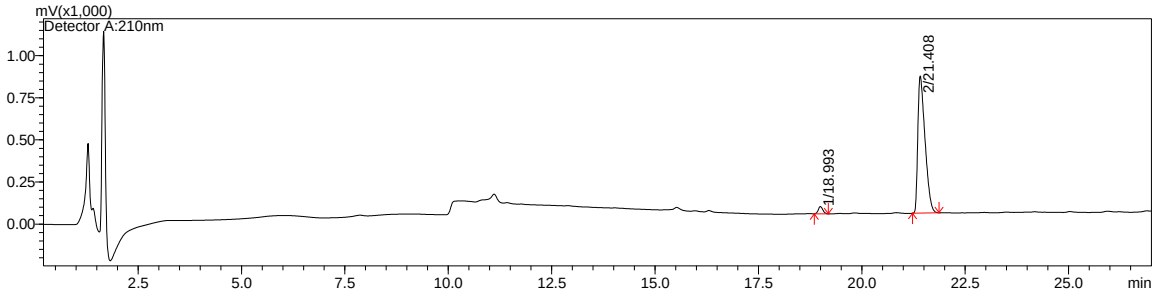

Figure SM-STAB-22. HPLC chromatogram of a [(*S*)-β^{2}hPhe^{4}]-TAPP (**17**) sample in human plasma, taken at 48 h of stability testing.